

# Influence of Plasma Spray Parameters on Formation and Morphology of $ZrO_2$ -8 wt% $Y_2O_3$ Deposits

Ahmet Kucuk,<sup>\*,†</sup> Rogerio S. Lima, and Christopher C. Berndt\*

Center for Thermal Spray Research, Department of Materials Science and Engineering,  
The State University of New York at Stony Brook, Stony Brook, New York 11794

Spray prints of thermal spray coatings were created on glass slides for air-plasma-sprayed 8-wt%-yttria-partially-stabilized zirconia (YSZ) deposits. The spray parameters such as carrier gas flow rate, standoff distance, and torch power were systematically changed to investigate the influence of these parameters on the YSZ deposit characteristics. The deposit properties such as deposition efficiency (DE), substrate coverage, deposit thickness, and roughness were measured. The deposits sprayed with a 3.5–4.0 L/min carrier gas flow rate at an 80 mm standoff distance exhibited higher values of DE within the range of studied process parameters. The DE increased as much as 25% by varying the carrier gas flow rate from 2.0 to 4.0 L/min. The deposits sprayed at a higher standoff distance and low torch power gave poor deposit characteristics. The deposit characteristics were compared with the in-flight particle parameters and revealed that the deposit characteristics strongly depended on the in-flight particle temperature. Using the in-flight particle properties, the flattening ratio and the splat thickness were calculated. The average size of particles adhering to the substrate was found to drastically change with a change of process conditions, being much less than the average size of the starting powder.

## I. Introduction

Thermal spray technologies such as high-velocity oxy-fuel, plasma, and flame spray processes have been widely used to provide metal, ceramic, and plastic coatings for various applications including wear resistance, heat insulation, and corrosion protection.<sup>1</sup> Yttria-partially-stabilized zirconia (YSZ) coatings have many applications as thermal barrier coatings in the aerospace and power generation industry.<sup>1</sup> A more thorough understanding of the thermal spray process and process variables is required to improve the characteristics of plasma-sprayed YSZ coatings.<sup>1–4</sup> Thermal spray coatings consist of microstructural units called splats, which form from the splashing of particles with high temperature and velocity on the substrate (Fig. 1). The in-flight particle parameters such as temperature and velocity determine droplet spreading and splat formation. Depending on in-flight characteristics, a particle will either stick on the substrate and form an adhered splat or bounce away from the substrate and not form a deposit. The quantity termed deposition efficiency (DE) indicates the percentage of particles that form splats within an

ensemble of particles arriving at the substrate. The splat morphology will also be reflected in the DE and, hence, determine the fashion in which splats build up during the coating formation process.

Recently, we have determined the in-flight parameters of YSZ particles in an air plasma environment for systematically varied spray conditions listed in Table I.<sup>4</sup> In the mentioned study, it was shown that the average temperature and velocity of YSZ particles either (i) gradually changed by changing their trajectory in the plasma jet via varying the carrier gas flow rate or (ii) drastically changed by varying the plasma operation conditions such as torch power, Ar/H<sub>2</sub> ratio, along with the standoff distance (Table II). In the current study, the deposits sprayed on glass slides using the same process parameters in the previous study<sup>4</sup> will be analyzed to gain an understanding of (i) splat formation and spreading, (ii) deposit buildup from individual splats, and (iii) the influence of in-flight particle characteristics (in turn, process variables) on the deposit morphology. The advantage in using the previous spray parameters is that they provide a broad average temperature and velocity range as well as systematically controlled gradually changing increments in the average particle temperature and velocity.

## II. Experimental Procedure

### (I) Sample Preparation

Yttria-partially-stabilized (8%) zirconia (YSZ) was atmospherically plasma sprayed on as-received glass microscope slides (Fisher Scientific, Pittsburg, PA) using a Metco 3MB plasma torch with a Metco GH nozzle (Sulzer Metco, Westbury, NY) mounted on a six-axis articulated robot (Model S400, GMF Fanuc, Charlottesville, VA). The feedstock was commercially available Metco 204NS-AE7590 powder with an average size of 80  $\mu\text{m}$  (Sulzer-Metco, Westbury, NY). A mechanical powder feeder was used to introduce the powder at a rate of 33 g/min into the plasma jet through a Metco No. 2 powder injector, which was vertically located 9 mm from the torch axis and 7 mm from the torch exit (Fig. 2). Details of the spray conditions are listed in Table I.

The as-received glass slides of 75 × 25 × 1 mm dimensions were cleaned with alcohol and air-dried prior to the spraying. The average surface roughness of microscope slides was less than

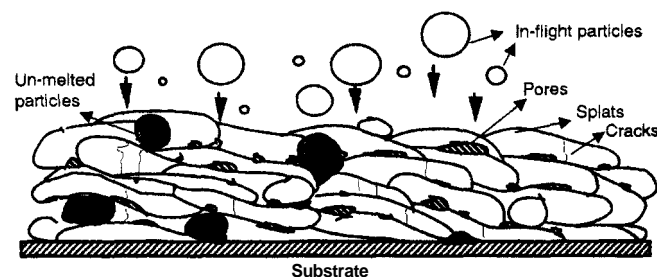


Fig. 1. Schematic microstructure of thermal spray coating consisting of splats, un-melted particles, pores, and cracks.

R. W. Rice--contributing editor

Manuscript No. 188682. Received March 27, 2000; approved November 10, 2000. Two of the authors (A.K. and C.C.B.) gratefully acknowledge financial support from the National Science Foundation under NSF-MRSEC DNR, Grant No. 9632570. One of the authors (R.S.L.) would like to acknowledge financial support from ONR Grant No. N00014-97-0843.

\*Member, American Ceramic Society.

†Present address: Karl Storz Endovision, Inc., Charlton, Massachusetts 01507.

Table I. Spray Parameters

Parameter	S-1	S-2	S-3	S-4	S-5	S-6
Current (A)	600	600	600	600	600	600
Voltage (V)	70	70	70	70	70	55
Primary gas, Ar (L/min)	40	40	40	40	50	50
Secondary gas, H <sub>2</sub> (L/min)	12	12	12	12	11	4.1
Powder carrier gas, Ar (L/min)	2.0	4.0	6.0	3.5	3.5	3.5
Standoff distance (mm)	80	80	80	80	100	100
Feeding rate (g/min)	33	33	33	33	33	33

Table II. Average Temperature and Velocity Values of In-Flight Particles at the Center-Line Location for the Given Conditions<sup>4</sup>

Sample/conditions	Average velocity (m/s)	Average temperature (°C)
S-1	130 ± 28	2432 ± 325
S-2	153 ± 35	2538 ± 373
S-3	148 ± 44	2524 ± 371
S-4	165 ± 73	2577 ± 446
S-5	156 ± 45	2326 ± 310
S-6	142 ± 37	2180 ± 267

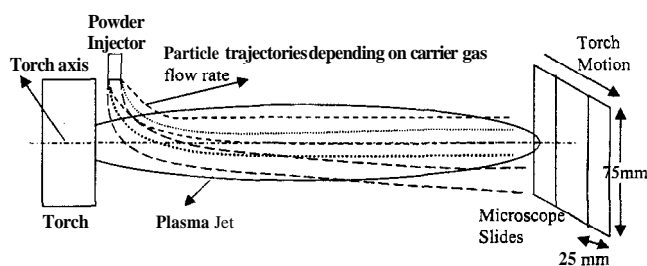


Fig. 2. Schematic of plasma spray systems with glass slide substrates. Note that the carrier gas flow rate changes the particle trajectory.

0.02  $\mu\text{m}$  with respect to the usual average roughness of a steel substrate used in such coatings being 5  $\mu\text{m}$ .<sup>2</sup> The glass slides were chosen as the substrate because they could provide consistent, reproducible surface conditions to spray on whereas the surface morphology of a grit-blasted substrate could drastically vary throughout the substrate. In addition, our experience showed that the surface morphology could not be easily reproduced for consequent grit blasting of the same metal substrate.

For each spray condition, three glass slides were placed onto the substrate holder in such a way that the width (25 mm) of the slide lay parallel to the direction of the torch motion (Fig. 2). The torch axis was approximately located at around the middle axis of the glass substrate. After the torch operation and the powder feeding were stabilized at given conditions (Table I), YSZ was sprayed in a single pass at a torch speed of 0.3 m/min.

### (2) Measurement of Physical Characteristics

The glass slides were weighed before and after the spraying using a Mettler Toledo AG balance (Fisher Scientific) with an accuracy of  $\pm 0.00001$  g. The DE of the process for each sample was calculated from Eq. (1)

$$DE = \frac{W_{\text{Deposited}}}{W_{\text{Injected}}} \times 100 \quad (1)$$

where  $W_{\text{Deposited}}$  is the weight of the YSZ deposit on the glass substrate, and  $W_{\text{Injected}}$  is the weight of the powder injected during the formation of the YSZ deposit.

The thicknesses of the deposits were measured throughout using a caliper with  $\pm 1$   $\mu\text{m}$  accuracy. The caliper anvils had a contact diameter of 6 mm.

The arithmetic mean roughness ( $R_a$ ) of the deposits was measured in the torch motion direction with a 2 mm interval throughout the 25 mm length using a Hommel T1000 mechanical profilometer (Hommel America, New Britain, CT). The roughness measurements were conducted with 0.5 mm/s traverse speed at 15 mm length.

### (3) Microscopy

A transmitted light microscope (Meiji, Island Park, NY) was used to determine the percentage coverage of the substrates by YSZ deposits. The representative images from an area of 3.5  $\text{mm}^2$  were recorded every 2.5 to 5 mm throughout the length of the microscope slide in the center of the slide width. Images 5 mm away from the center of a slide width were also taken, and it was ascertained that the substrate coverage did not change within the experimental errors throughout the width for a given distance from the top of the slide. Therefore, only values determined from the width center were represented in the current study.

## III. Results

### (1) Deposition Efficiency

Figure 3 illustrates the DE calculated for the different spray conditions. It ranged from 7% to 25%. The DE values reported in the open literature were in the range of 20% to 50% for the plasma-sprayed YSZ in industrial processes (Table III). The differences in the DE values in the current study and the open literature DE values were due to the use of glass slide substrates with an average roughness less than 0.02  $\mu\text{m}$  in the current study versus use of a metallic substrate with an average roughness greater than 5.0  $\mu\text{m}$  in the industrial processes. The DE at a spray distance of 80 mm first increased with increasing carrier gas flow rate and then decreased for a carrier gas flow rate of 6 L/min. The DE increased as much as 25% by varying the carrier gas flow rate from 2.0 to 3.5 L/min. As shown in Fig. 3, the DE drastically

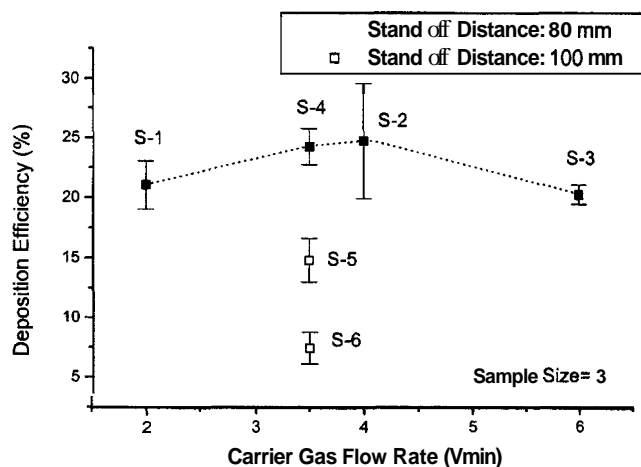


Fig. 3. Change of deposition efficiency (DE) with the plasma spray variables.

Table III. Comparison of the Deposition Efficiency for Different Plasma Spray Systems

DE (%)	Process conditions	Ref.
40–65	Miller SG-100, 900 A, 34 V, 47 L/min Ar, 22.2 L/min He, 11 m/s injection velocity, S.D.: 50–120 mm, zirconia (AI-1075)	17
40–60	No value on torch parameters, with a NiCrAlY bond coat, S.D.: 75–120 cm, 30–62 $\mu\text{m}$ , spherical, hollow sphere or aggregates	20
55	Miller SG-100, 800 A, 34–42 V, 50 L/min Ar, 2 L/min $H_2$ , 6.5 L/min Ar, 23 g/min, S.D.: 63 mm, grit-blasted mild steel substrate, fused YSZ with $-45 + 22 \mu\text{m}$	19
42–56	Plasmatechnik A3000S, 610 A, 73 V, 41 L/min Ar, 14 L/min $H_2$ , 1.3 m/s injection velocity, 21–37 g/min, S.D.: 110 mm, grit-blasted steel, fused crushed $Al_2O_3$ (Amperit 740.1)	18
48–51	Metco 3MB, 500–600 A, 40 L/min Ar, 7–12 L/min $H_2$ , 5–6 L/min Ar, 20 g/min, S.D.: 100 mm, grit-blasted steel, crushed YSZ with 41–110 $\mu\text{m}$	15
51–60	Metco 3MB, 500–600 A, 40 L/min Ar, 7–12 L/min $H_2$ , 5–6 L/min Ar, 20 g/min, S.D.: 100 mm, grit-blasted steel, hollow sphere YSZ with 30–99 $\mu\text{m}$	15
19	Sulzer-Metco F4-MB, 475 A, 66 V, 42 L/min Ar, 9 L/min $H_2$ , 1.7 L/min, 35 g/min, S.D.: 140 mm, grit-blasted Inconel 625 with a bond 200 $\mu\text{m}$ bond coat, YSZ	16
44	Sulzer-Metco F4-MB, 605 A, 70 V, 37 L/min Ar, 12 L/min $H_2$ , 1.3 L/min, 35 g/min, S.D.: 140 mm, grit-blasted Inconel 625 with a bond 200 $\mu\text{m}$ bond coat, YSZ	16
52	Sulzer-Metco SM-F100, 450 A, 41 V, 42 L/min Ar, 4 L/min $H_2$ , 2.5 L/min, 35 g/min, S.D.: 70 mm, grit-blasted Inconel 625 with a bond 200 $\mu\text{m}$ bond coat, YSZ	16
28	Sulzer-Metco SM-F100, 350 A, 38 V, 42 L/min Ar, 2 L/min $H_2$ , 2.5 L/min, 35 g/min, S.D.: 70 mm, grit-blasted Inconel 625 with a bond 200 $\mu\text{m}$ bond coat, YSZ	16
39–49	TAFA 7070 PlazJet, 420–500 A, 185–235 L/min $N_2$ , 85–105 L/min $H_2$ , 160–200 g/min, S.D.: 140–180 mm, sand-papered Hastelloy X ( $R_a = 1 \mu\text{m}$ ) with 200 $\mu\text{m}$ NiCoCrAlY bond coat, YSZ (Amperit 827.090) with $-45 + 10 \mu\text{m}$	21
51	500 A, 78 V, 50 Ar L/min, 11 L/min $H_2$ , 23 g/min, S.D.: 100 mm, as-received Ni-based alloy with 125 $\mu\text{m}$ NiCoCrAlY bond coat, YSZ (Starck 821)	22
50	TAFA HPPS Plazjet, 400–500 A, 300–400 V, 130–210 L/min $N_2$ , 48–95 L/min $H_2$ , 140–260 g/min, S.D.: 100–200 mm, as-received Ni-based alloy with 125 $\mu\text{m}$ NiCoCrAlY bond coat, YSZ (Starck 821)	22
7–25	Metco 3MB, 600 A, 55–70 V, 40–50 L/min Ar, 11–12 L/min $H_2$ , 2–6 L/min Ar, 33 g/min, S.D.: 80–100 mm, glass slides with $R_a = 0.02 \mu\text{m}$ , YSZ	This

lowered with increasing standoff distance and Ar/ $H_2$  ratio along with decreasing torch power.

(2) Roughness Profiles

The average roughness profiles for the samples sprayed with varying parameters are given in Fig. 4. The position where the average roughness was the highest shifted with increasing carrier gas flow rate to a lower portion of the microscope slide (i.e., notice the progression to the right for samples S-1, S-2, and S-3), whose top edge is the origin (Fig. 4(a)). While the average roughness ( $R_a$ ) values were similar for the deposits formed at 80 mm standoff distance, R, decreased going from sample S-4 to S-6, all of which were sprayed using a carrier gas flow rate of 3.5 L/min. The position of the highest  $R_a$  was similar (at around 33 mm) for samples S-4, S-5, and S-6. The bell-shaped  $R_a$  profiles were asymmetric with respect to their centers.

(3) Thickness Profiles

The average thickness profiles of the deposits are presented in Fig. 5. The profiles for the samples sprayed at 80 mm were similar except for the position of the maximum thickness. The position shifted to a lower portion of the substrate with increasing carrier gas flow rate. The maximum thickness varied from 50 to 15  $\mu\text{m}$  depending on the spray parameters. The average thickness profiles (Fig. 5) and the average roughness profiles (Fig. 4) were similar; i.e., the bell-shaped profiles were located at the same position within the experimental errors.

(4) Substrate Coverage Profiles

A macroscopic view of a representative slide from each spray condition taken by a digital camera is presented in Fig. 6. As shown, the position of the spray prints (in black) shifted to a lower portion of the slides with increasing carrier gas flow rate, taking into account that samples S-5 and S-6 were not sprayed under the same plasma parameters. The image in Fig. 6 also revealed that the morphology of the deposits was different. Deposit S-6, for instance, was spread over a larger area, but with a less dense

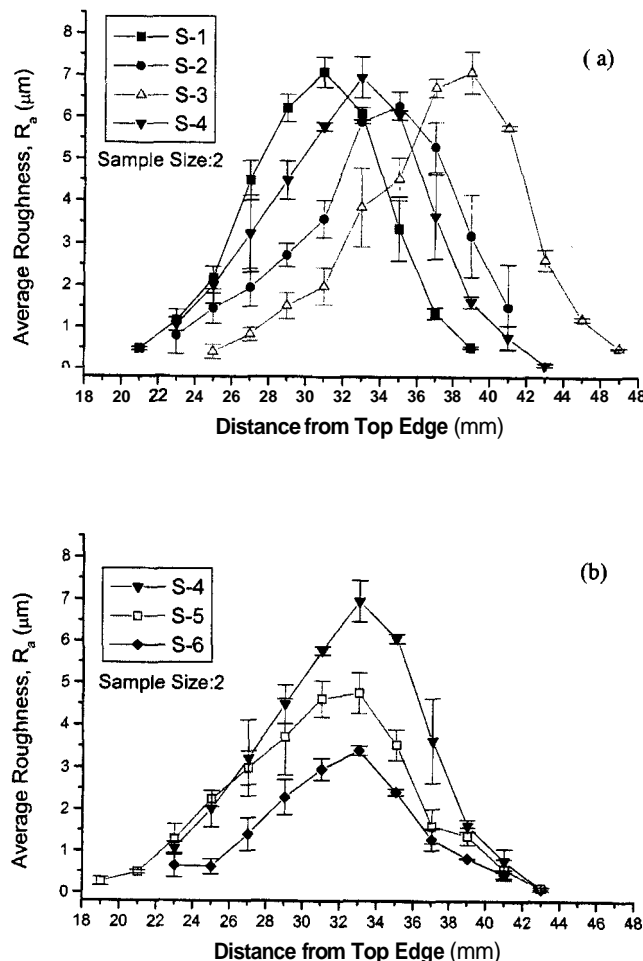


Fig. 4. Average roughness profiles for the deposits sprayed (a) at 80 mm standoff distance, and (b) with a carrier gas flow rate of 3.5 L/min.

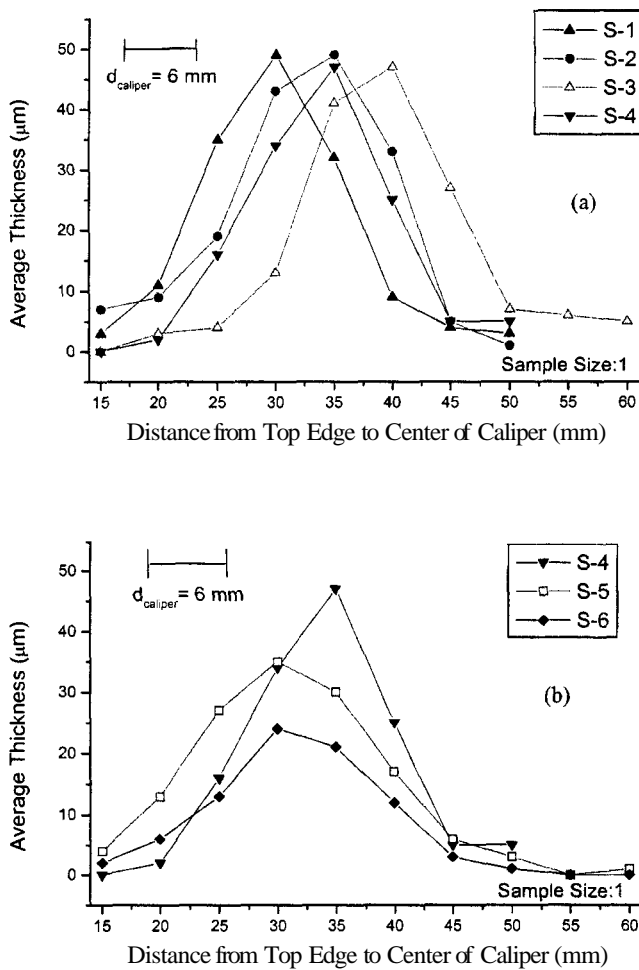


Fig. 5. Average thickness profiles for the deposits sprayed (a) at 80 mm standoff distance, and (b) with carrier gas flow rate of 3.5 L/min. Note that the position in the "x" axis represents the middle of the caliper anvil.

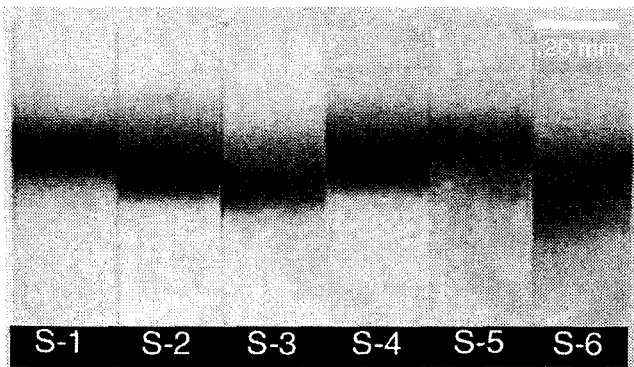


Fig. 6. Picture of six representative slides for each spray condition. Note that dark areas are the YSZ deposit on the microscope slides.

formation. Figure 7 illustrates more detailed images of the deposits taken using a transmitted light microscope. The numbers on the left represent the position where micrographs were taken and dark regions in these images indicate the areas covered by YSZ splats. The percentage substrate coverage, which was calculated from the micrographs presented in Fig. 7, is given in Fig. 8 for each spray condition. As shown, the maximum coverage was as high as 90% for samples S-1, S-2, and S-4, while others (S-3, S-5, S-6) had maximum substrate coverage of 50% to 80% depending on the spray conditions. The readers should be cautioned here that DE and percentage substrate coverage are two different quantities and higher substrate coverage does not necessarily mean higher DE.

The substrate coverage profiles were bell-shaped and similar to the roughness and thickness profiles (Figs. 4 and 5). The position of maximum coverage shifted to the lower portion of the slides with increasing carrier gas flow rates for a given standoff distance (80 mm) (Figs. 6–8). Even though the substrate coverage was low for samples S-5 and S-6, their spray prints were broader with respect to samples sprayed at 80 mm standoff distance (Fig. 8).

#### IV. Discussion

##### (1) Splat Formation and Spreading

When high-velocity, high-temperature molten/semimolten particles encounter a substrate in a thermal spray process, they spread and solidify to form microstructural units called splats. Various aspects of droplet spreading and splat formation have been studied by several researchers.<sup>5–10</sup> Madejski<sup>9</sup> formulated the spreading of molten droplets as follows:

$$\frac{D_s}{a_p} = 1.2941 \left( \frac{\rho v d_p}{\eta} \right)^{0.2} = 1.2941 \text{Re}^{0.2} \quad (2)$$

where  $D_s$  is the splat diameter,  $d_p$  is the particle (droplet) diameter,  $\rho$  is the density,  $v$  is the particle velocity,  $\eta$  is the kinetic viscosity, and  $\text{Re}$  is the Reynolds number. The ratio  $D_s/d_p$  is defined as the flattening ratio ( $f_p$ ). In addition to Madejski, other researchers have proposed similar formulas for the formation of splats except that they have replaced the coefficients with different numbers from 0.83 to 1.054 for 1.294 and 0.125 to 1.0 for 0.2.<sup>5</sup> However, Vardelle *et al.*<sup>5</sup> showed that the experimentally determined flattening ratio for plasma sprayed YSZ on a polished stainless steel substrate was in good agreement with the flattening ratio calculated from the Madejski equation (Eq. (2)).

Since the in-flight particle characteristics for each spray condition were known in the current study (Table II),<sup>4</sup> it was possible to estimate the flattening ratio for the splats, which were located around the center line, under different spray conditions using the Madejski equation. In the equation, the density of YSZ particles was taken to be 5700 kg/m<sup>3</sup> as Vardelle *et al.*<sup>5</sup> did, while kinetic viscosity was calculated from  $\eta$  (Pa·s) = 0.1 exp(-2.95 + 5993/ $T_p$ ), where  $T_p$  is the particle temperature in kelvins.<sup>7</sup> In the calculations, only particles with temperatures equal to or higher than 2700°C (melting point of YSZ) were taken into consideration. The particle temperature, velocity, and size values were obtained from the previous study.<sup>4</sup>

The estimated average flattening ratios along with particle and splat diameters and splat thickness are given in Fig. 9. The splat thickness was calculated from the flattening ratio by assuming that splats had a regular disk shape. The average flattening ratio was around 5.5 (varied in the range of 4.8 to 6.2) with an average splat thickness of around 1.0 μm (varied in the range of 0.5 to 1.5 μm), while the average particle and splat diameters ranged in 35–55 μm and 180–300 μm intervals, respectively, depending on the spray conditions. Vardelle *et al.*<sup>5,6</sup> reported that the flattening ratio for air-plasma-sprayed YSZ with 22–45 μm size on polished stainless steel varied from 3.5 to 5.5. In addition, Leger *et al.*<sup>11</sup> measured the average flattening ratios for air-plasma-sprayed YSZ with similar size distributions on steel and zirconia substrates to be 4.9 and 4.7, respectively. They also found that the average flattening ratio decreased with increasing substrate roughness. Bianchi *et al.*<sup>12</sup> reported that the average flattening ratio and the average splat thickness for air-plasma-sprayed YSZ (+22–45 μm) on a preheated stainless substrate with 0.2 μm roughness are 5.0 and 0.85 μm, respectively. When they increased the size of the nozzle from 7 to 10 mm, these values changed to 4.6 and 1.1, respectively. Jiang *et al.*<sup>13</sup> found that YSZ splats sprayed on a stainless steel substrate, which was preheated to 400°C, exhibited a flattening ratio ranging from 3.0 to 5.0 with an average value of 4.0, and a splat thickness ranging from 0.4 to 1.8 μm with an average value of 1.0 μm.

All of these values (Table IV) reported in the open literature are in good agreement with each other within the experimental

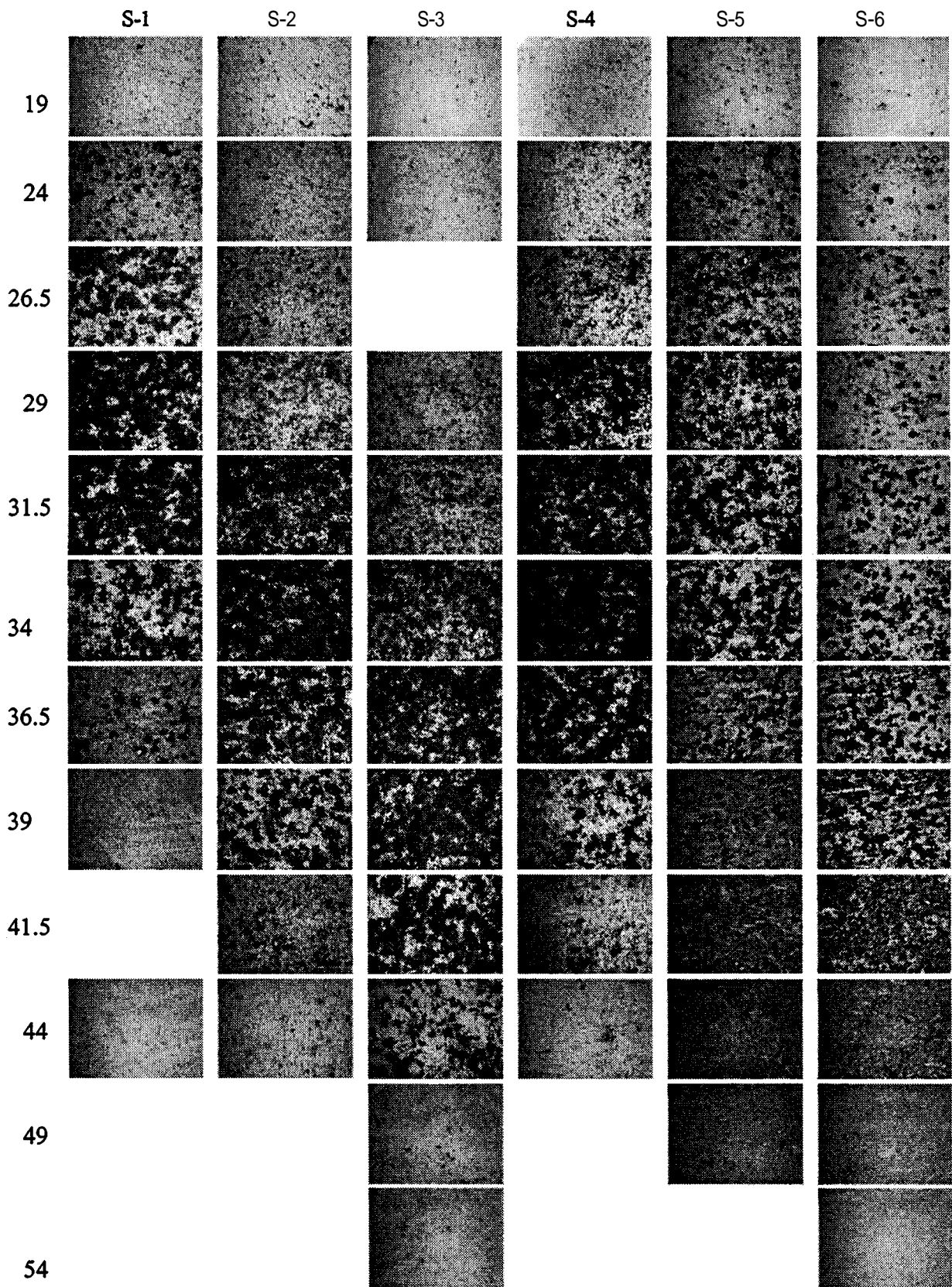


Fig. 7. Transmitted light microscope images of deposits. The number on the left is the distance between the top edge of the slide and the middle of the area ( $3.5 \text{ mm}^2$  where image is taken). The width of each image is about 2 mm. The dark areas represent the YSZ deposit.

variations such as measurement technique and spraying practice. In all of these studies, it was indicated that a preheated smooth substrate was required to obtain splats with regular shapes (perfect disk shape). When the substrate temperature was low, such as room temperature, splat shapes were distorted (some fragmented)

and shaped more like a flower. In the current study, the morphology of splats was mostly irregularly disk-shaped (Fig. 7). Nevertheless, the estimated flattening ratio and the splat thickness from the Madejksi equation (Eq. (2)) in the current study were in good agreement with the experimental results summarized above within

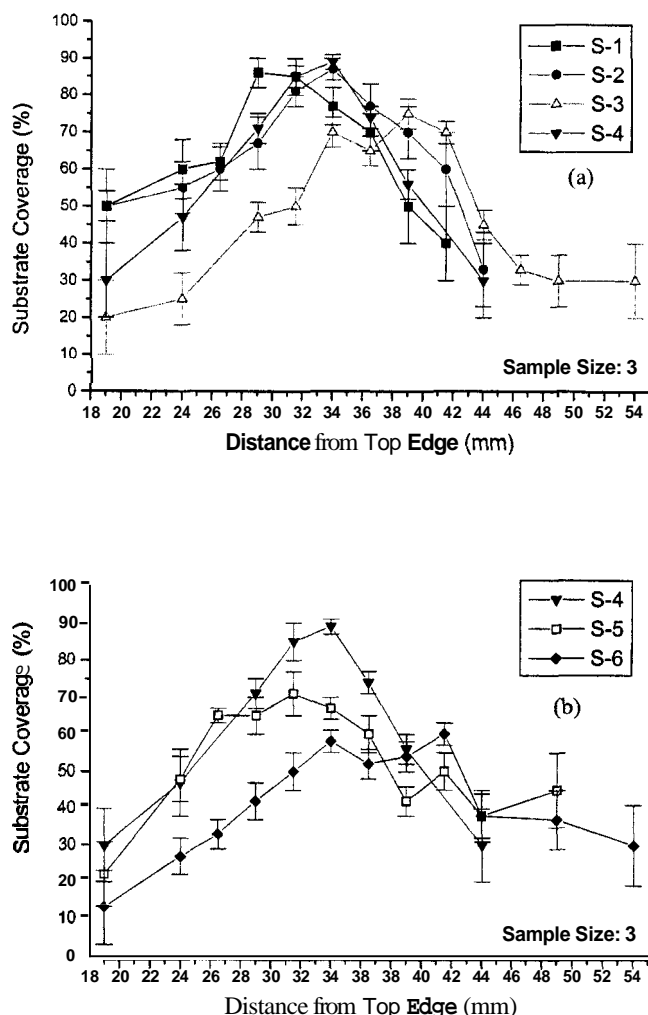


Fig. 8. Profiles of percentage substrate coverage for the deposits sprayed (a) at 80 mm standoff distance, and (b) with carrier gas flow rate of 3.5 L/min. The values calculated from the images presented in Fig. 6.

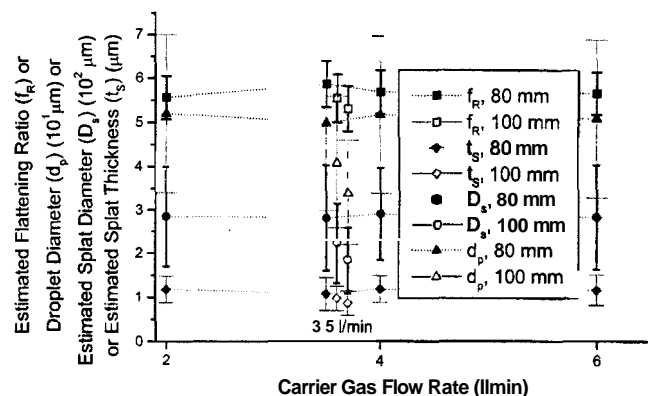


Fig. 9. Change of flattening ratio, droplet and splat diameters, and splat thickness with the spray conditions. The values were calculated using the Madjecki equation (Eq. (2)).

the limits of errors. The splat diameters calculated in the current study seemed higher than the values reported in the open literature. However, the particle size values in the previous study were lower.

As shown in Fig. 9, the estimated splat characteristics slightly changed for the deposits sprayed at a standoff distance of 80 mm. However, the deposits sprayed using a lower power or a higher  $Ar/H$  ratio at a standoff distance of 100 mm revealed lower average values for the splat characteristics because the average

particle temperature was low for those sprayed at 100 mm (Table II). A lower average particle temperature allows only smaller particles to be melted (and/or semimelted). It should be noted here that the average particle (droplet) size ranged from 35 to 55  $\mu\text{m}$  while the average particle size of the feedstock was 80  $\mu\text{m}$ . Therefore, larger particles most likely bounce away from the substrate rather than forming a coherent deposit.

## (2) Deposit Characteristics

As shown in Figs. 4–8, each slide exhibited a distinct spray print characteristic. The position of the spray print (deposit) shifted to a lower portion of the slide with increasing carrier gas flow rate while it was broadened and less densely covered with increasing spray distance and decreasing torch power. All of these results agreed with the in-flight characteristics of the processes presented previously: and summarized in Table II. In the previous study,<sup>4</sup> it was shown that the penetration of the injected particle into the plasma jet, and then acceleration of this particle, depended on the injection velocity (i.e., carrier gas flow rate). The vertical distance traveled by a particle (penetration) was found to increase with an increasing carrier gas flow rate. In the previous study: it was also shown that the center-line position, where particle flux is the highest, moved to a lower portion of the spray jet with increasing carrier gas flow rate as a result of the higher vertical distance traveled. Therefore, it was reasonable that such shifting bell-shaped profiles (Figs. 4–8) were observed for samples S-1 to S-4 since the carrier gas flow rate increased gradually.

The spray print size was larger for the samples deposited at higher standoff distances (S-5 and S-6) (Figs. 4–8) because (i) the plasma jet widens with increasing distance from the torch for a given spray properties and (ii) the width of the plasma jet changes with the spray parameters. The center of the bell-shape property curves (Figs. 4–8) was located at a similar position for samples S-4, S-5, and S-6, which were sprayed using the same carrier gas flow rate.

## (3) Deposition Efficiency

The DE presented in Fig. 3 was in good agreement with the expected values from the in-flight characteristics. In the previous study: it was suggested that DE in a plasma spray process depends on the in-flight particle characteristics, especially the percentage of particles (moltdsemimolten) with a temperature higher than the melting point of YSZ. It was found that the percentage of moltdsemimolten particles was 19%, 33%, 30%, 35%, 11%, and 3% for samples S-1 to S-6 in the center-line position, respectively. Similarly, the DE values in Fig. 3 were 21%, 25%, 20%, 24%, 15%, and 7% for samples S-1 to S-6, respectively. Although the trends in the DE values and the percentage of molten/semimolten particles were similar, the absolute values differed. However, one should consider the percentage of molten/semimolten particles throughout the spray jet as well as that in the center line since the DE value presented in Fig. 3 represented the quantity throughout the deposit. In the previous study, it was shown that percentage of moltdsemimolten particles decreased for samples S-2, S-3, and S-4 at the position away from the center line, while it increased for samples S-1, S-5, and S-6 at lower vertical positions of the spray jet (i.e., below the center line). Therefore, the discrepancy presented above between the DE values and the percentage of moltdsemimolten particles could be closed when the particles at other positions (other than the center line) were considered. As expected, the DE for S-2, S-3, and S-4 was lower than the percentage of moltdsemimolten particles at the center line, while the DE for S-1, S-5, and S-6 was higher than the percentage of molten/semimolten particles at the center line. However, these two values became similar when an average percentage of moltdsemimolten particles was taken throughout the deposits. As a result, the DE in a plasma spray process strongly depends on the temperature of the particles in flight.

The deposit characteristics such as thickness, substrate coverage, and roughness were a reflection of the DE; i.e., the higher the DE, the higher the values of the deposit characteristics. It was

**Table IV. Flattening Ratio and Splat Thickness Values for Plasma-Sprayed YSZ Splats Reported in the Open Literature**

$f_R$	$t_s$ ( $\mu\text{m}$ )	Process conditions	Method	Ref.
4.2–4.9		Atmospheric plasma torch, 600 A, 73 V, 45 L/min Ar, 15 L/min H <sub>2</sub> , 3 g/min, S.D.: 120 mm, stainless steel ( $R_a = 0.05, 0.4, \text{ or } 9 \mu\text{m}$ ) and zirconia ( $R_a = 0.2 \text{ or } 4 \mu\text{m}$ ) substrate, $T_s$ : 350–400°C, YSZ with 22–45 $\mu\text{m}$	Pyrometer during particle impact, profilometer microscopy	11
	0.6–1.9	Atmospheric torch, 600 A, 62 V, 45 L/min Ar, 15 L/min H <sub>2</sub> , 4 L/min Ar, 17 g/min, S.D.: 100 mm, cast iron-and stainless steel ( $R_a = 0.2 \text{ or } 12 \mu\text{m}$ ), $T_s$ : 75–300°C, YSZ with 45 $\pm$ 22 $\mu\text{m}$		23
4.6–5.0	0.85–1.1	Atmospheric plasma torch, 600 A, 45 L/min Ar, 15 L/min H <sub>2</sub> , 3.5–4.5 L/min Ar, 0.2 g/min, S.D.: 100 mm, stainless steel ( $R_a = 0.1 \mu\text{m}$ ), $T_s$ : 75° or 300°C, YSZ 45 $\pm$ 22 $\mu\text{m}$	Pyrometer during particle impact	12
3.6	2.4	Tekna PL50 rf plasma torch, 47 kW, central gas, Ar: 50 L/min, sheath gas: 90 Ar + 10 H <sub>2</sub> L/min, 3.0 L/min, 0.2 g/min, S.D.: 270 mm, stainless steel ( $R_a = 0.1 \mu\text{m}$ ), $T_s$ : 75° or 300°C, YSZ 45 $\pm$ 22 $\mu\text{m}$	Pyrometer during particle impact	12
3.5–5.5		Atmospheric plasma torch, 400–600 A, 53–55 V, 27–45 L/min Ar, 7–15 L/min H <sub>2</sub> , 1.5–8 L/min Ar, S.D.: 100 mm, stainless steel ( $R_a = 0.1 \mu\text{m}$ ), $T_s$ : 75° or 300°C, YSZ 45 $\pm$ 22 $\mu\text{m}$	Pyrometer during particle impact	6
4 (3–5)	1.0 (0.4–1.8)	Plasma Technik PT-F4, 600 A, 78 V, 40 L/min Ar, 12 L/min H <sub>2</sub> , S.D.: 100 mm, stainless steel ( $R_a = 0.1 \mu\text{m}$ ), $T_s$ : 400°C, YSZ with 33 $\mu\text{m}$	Profilometer	13
3.8	1.1	Plasma Technik PT-F4, 600 A, 60 V, 45 L/min Ar, 15 L/min H <sub>2</sub> , 3.5 L/min Ar, S.D.: 100 mm, stainless steel ( $R_a = 0.1 \mu\text{m}$ ), $T_s$ : 300°C, YSZ with 33 $\mu\text{m}$	Profilometer	24
5–6	0.8–1.2	Metco 3MB, 600 A, 55–70 V, 40–50 L/min Ar, 11–12 L/min H <sub>2</sub> , 2–6 L/min Ar, 33 g/min, S.D.: 80–100 mm, glass slides with $R_a = 0.02 \mu\text{m}$ , YSZ	Calculated from Madejki equation	This

possible to estimate the comparable (relative) mass of the YSZ deposited throughout the coating since the thickness and substrate coverage were known throughout the deposit. The relative mass of the YSZ deposit was calculated from the following equation:

$$W_{\text{YSZ}} = \frac{(\%C) A_T t_D \rho_{\text{YSZ}}}{100} \quad (3)$$

where %C is the percentage substrate coverage, A, is the area (3.5 mm<sup>2</sup>) where an image was taken for substrate coverage analysis,  $t_D$  is the thickness of the deposit, and  $\rho_{\text{YSZ}}$  is the density of YSZ, taken as 6.0 g/cm<sup>3</sup>.<sup>14</sup>

The estimated relative mass,  $W_{\text{YSZ}}$ , throughout the deposit for each spray condition is presented in Fig. 10. The total relative mass of the deposit was calculated by integrating the area under each curve in Fig. 10. The estimated total relative mass was 10.0, 11.3, 8.6, 9.4, 7.2, and 3.6 mg for samples S-1 to S-6, respectively. Strikingly, the measured mass of the deposits changed  $9.6 \pm 0.9$ ,  $11.3 \pm 2.1$ ,  $9.2 \pm 0.4$ ,  $11.0 \pm 0.7$ ,  $6.8 \pm 0.8$ , and  $3.4 \pm 0.6$  mg for S-1 to S-6, respectively. Therefore, the relative estimated mass could be used as a quantity to compare the mass of the deposits at different position in the coating (Fig. 10).

**(4) Comparison with Previous Deposition Efficiency Data**

The DE values for plasma-sprayed YSZ in various industrial processes along with the current study are listed in Table III. In Table III, the process conditions (torch type, current, voltage, primary and secondary gas flow rates, carrier gas flow rate, powder injection velocity, substrate conditions, standoff distance (S.D.), and feedstock characteristics) are also given whenever possible with the order listed. The DE values ranged from 19% to

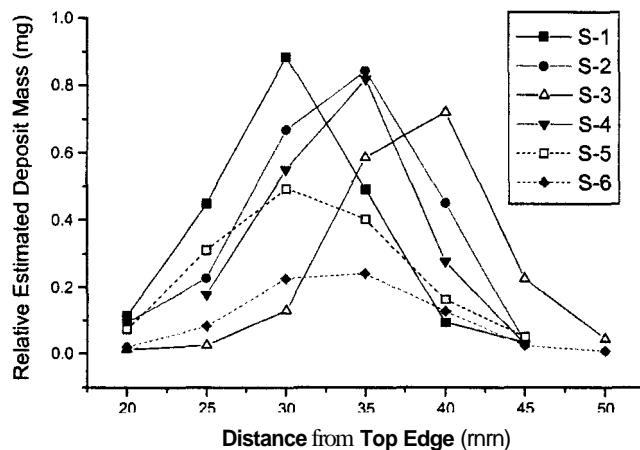


Fig. 10. Relative estimated deposit mass throughout the deposits for different spray conditions. Note that these values should be taken as comparable values rather than absolute values.

65% depending on the process conditions in the industrial processes while they varied from 7% to 25% in the current study. As mentioned, the difference arose from the use of a glass substrate with low roughness (less than 0.02  $\mu\text{m}$ ) in the current study with respect to the metal substrate with more than 5  $\mu\text{m}$  average roughness in the industrial processes. A rougher surface enhances DE due to improved mechanical adhesion between the substrate and the splat resulting from impinging. In addition, it also creates a rougher surface with respect to use of a smooth glass substrate for the secondary splats arriving on the top of the first splat layer.

Furthermore, other factors such as heat conduction differences, deformability due to impacting particles, local melting/softening near the substrate surface, and oxidation/crystallization should be considered in the comparison of a metallic substrate and a glass slide.

For a YSZ coating<sup>17</sup> sprayed on a grit-blasted steel substrate using the same plasma torch with similar process parameters in the current study (Table I), the DE was 60% versus 21% for the deposit sprayed on the glass slide in the current study. Nevertheless, it is believed that the DE determined using a glass slide provides comparable values to investigate the influence of spray parameters.

The general conclusions below could be drawn from the references included in Table III. The DE was lower for the deposits sprayed (i) with a lower torch power,<sup>15,16</sup> (ii) at a larger standoff distance,<sup>17</sup> (iii) with an older (worn) torch electrode,<sup>18,19</sup> and (iv) with a higher powder feed rate.<sup>17</sup> The porosity in YSZ coatings increased with the decreasing DE.<sup>17</sup> In addition, DE also varied with the powder morphology: A hollow sphere YSZ feedstock with high crust density, for instance, yielded a higher DE than crushed YSZ<sup>15</sup> because hollow sphere particles provide more uniform temperature distribution. One may expect that the temperature distribution in an irregularly shaped crushed particle would be less homogeneous than that in a regularly shaped spherical particle. Similarly, a spray-dried porous feedstock would yield a lower DE since the heat could not transfer to inner layers easily.

## V. Conclusions

The YSZ spray prints created on glass slides using various process parameters were examined using optical microscopy, profilometry, and an electronic balance. It was found that the DE, roughness, percentage substrate coverage, and thickness of the deposits depended on the process parameters.

The profiles for average roughness, average thickness, and percentage substrate coverage values throughout the deposits were obtained. These bell-shaped profiles shifted position on the slide depending on the carrier gas flow rate. The values in the profiles were controlled by the in-flight particle characteristics.

The Madjeski equation (Eq. (2)) was used to estimate the flattening ratio, splat thickness, and diameter. The values calculated were in good agreement with the previous experimental studies and the values determined by optical microscopy in the current study. Although the average flattening ratio (around 5.5 with a variation range of 4.8 to 6.2) and splat thickness (around 1.0  $\mu\text{m}$  with a range of 0.5 to 1.5  $\mu\text{m}$ ) values were not dramatically different within the limits of errors for the samples deposited with different spray parameters, it was found that the average size of the particles, which adhere and formed a splat, decreased with decreasing average in-flight particle temperature. The highest average particle size adhered was around 52  $\mu\text{m}$  with respect to the average starting particle size of 80  $\mu\text{m}$ . Therefore, use of a feedstock with smaller particle size would improve DE drastically. One should caution that there is a limit for the smallest particle size that can be used since small particles may not have enough momentum to penetrate into the plasma jet, but bounce away.

The DE varied from 7% to 25% depending on the spray conditions. Even though the DE range found in the current study was lower than the range in industrial processes (20% to 65%) due to the use of smooth glass slides versus grit-blasted metallic substrates, the DE values in the current study served well for comparison of different spray parameters. A strong correlation between in-flight particle temperature and DE was found. The percentage of molten/semimolten particles among the particles arriving at the substrate determined the DE: the higher the percentage, the higher the DE.

## References

<sup>1</sup>L. Pawlowski, *The Science and Engineering of Thermal Spray Coating*. Wiley, New York, 1995.

<sup>2</sup>A. Kucuk, C. C. Berndt, U. Senturk, and R. S. Lima, "Influence of Plasma Spray Parameters on Mechanical Properties of Yttria Stabilized Zirconia Coatings. II: Acoustic Emission." *Mater. Sci. Eng. A*, in press.

<sup>3</sup>A. Kucuk, C. C. Berndt, U. Senturk, R. S. Lima, and C. R. C. Lima, "Influence of Plasma Spray Parameters on Mechanical Properties of Yttria Stabilized Zirconia Coatings. I: Four Point Bend Test," *Mater. Sci. Eng. A*, in press.

<sup>4</sup>A. Kucuk, R. S. Lima, and C. C. Berndt, "Influence of Plasma Spray Parameters on In-Flight Characteristics of  $\text{ZrO}_2$ -8 wt%  $\text{Y}_2\text{O}_3$  Ceramic Particles," *J. Am. Ceram. Soc.*, **84** [4] 685–92 (2001).

<sup>5</sup>M. Vardelle, A. Vardelle, A. C. Leger, and P. Fauchais, "Dynamics of Splat Formation and Solidification in Thermal Spraying Processes"; pp. 555–62 in *Thermal Spray Industrial Applications*. Edited by C. C. Berndt and S. Sanjay. ASM International, Materials Park, OH, 1994.

<sup>6</sup>M. Vardelle, P. Fauchais, A. Vardelle, and A. C. Leger, "Influence of the Variation of Plasma Torch Parameters on Particle Melting and Solidification"; pp. 535–41 in *Thermal Spray: A United Forum for Scientific and Technological Advances*. Edited by C. C. Berndt. ASM International, Materials Park, OH, 1997.

<sup>7</sup>V. V. Sobolev and J. M. Guilemany, "Flattening of Droplets and Formation of Splats in Thermal Spraying: A Review of Recent Work—Part 2" *J. Therm. Spray Technol.*, **8** [2] 301–4 (1999).

<sup>8</sup>V. V. Sobolev and J. M. Guilemany, "Flattening of Droplets and Formation of Splats in Thermal Spraying: A Review of Recent Work—Part 1," *J. Therm. Spray Technol.*, **8** [1] 87–101 (1999).

<sup>9</sup>J. Madjeski, "Solidification of Droplets on a Cold Substrate," *Int. J. Heat Mass Transfer*, **19**, 1009–13 (1976).

<sup>10</sup>H. Fukunuma and A. Ohmori, "Behavior of Molten Droplets Impinging on Flat Surfaces"; pp. 563–68 in *Thermal Spray Industrial Applications*. Edited by C. C. Berndt and S. Sampath. ASM International, Materials Park, OH, 1994.

<sup>11</sup>A. C. Leger, M. Vardelle, A. Vardelle, B. Dussoubs, and P. Fauchais, "Splat Formation: Ceramic Panicles on Ceramic Substrate"; pp. 169–74 in *Thermal Spray Science and Technology*. Edited by C. C. Berndt and S. Sampath. ASM International, Materials Park, OH, 1995.

<sup>12</sup>L. Bianchi, P. Lucchese, A. Denoirjean, and P. Fauchais, "Zirconia Splat Formation and Resulting Coating Properties"; pp. 261–66 in *Thermal Spray Science and Technology*. Edited by C. C. Berndt and S. Sampath. ASM International, Materials Park, OH, 1995.

<sup>13</sup>X. Jiang and S. Sampath, "Effect of Substrate Condition on Splat Formation During Thermal Spray Deposition"; pp. 439–48 in *Solidification 1998*. Edited by S. P. Marsh, J. A. Dantzig, W. Hofmeister, R. Trivedi, M. G. Chu, E. J. Lavernia, and J. H. Chun. The Minerals, Metals and Materials Society, Warrendale, PA, 1998.

<sup>14</sup>R. Stevens, "Engineering Properties of Zirconia"; pp. 775–86 in *Engineered Materials Handbook*, Vol. 4, *Ceramics and Glasses*. ASM International, Materials Park, OH, 1991.

<sup>15</sup>T. J. Jewett, W. C. Smith, H. Herman, J. Margolies, and S. Sampath, "Plasma Processing of Functionally Graded Materials. Part II: Deposit Formation"; pp. 607–12 in *Thermal Spray: A United Forum for Scientific and Technological Advances*. Edited by C. C. Berndt. ASM International, Materials Park, OH, 1998.

<sup>16</sup>L. Leblanc, C. Moreau, J.-G. Legoux, and B. Arsenault, "Characterization of Plasma Spray Processes by Monitoring the State of the Sprayed Particles"; pp. 329–34 in *United Thermal Spray Conference—1999*, Edited by E. Lugscheider and P. A. Kammer. German Welding Society, Dusseldorf, Germany, 1999.

<sup>17</sup>J. R. Fincke and W. D. Swank, "Air-Plasma Spraying of Zirconia: Spray Characteristics and Standoff Distance Effect on Deposition Efficiency and Porosity"; pp. 513–18 in *Thermal Spray: International Advances in Coating Technology*. Edited by C. C. Berndt. ASM International, Materials Park, OH, 1992.

<sup>18</sup>J. Knuutila, P. Saarenrinne, R. Hernberg, T. Lehtinen, and T. Mäntylä, "In-Situ Measurement of Particle Concentration and Velocity Using a Non-Intensified CCD Camera"; pp. 577–82 in *Thermal Spray: A United Forum for Scientific and Technological Advances*. Edited by C. C. Berndt. ASM International, Materials Park, OH, 1997.

<sup>19</sup>L. Leblanc, P. Gougeon, and C. Moreau, "Investigation of the Long-Term Stability of Plasma Spraying by Monitoring Characteristics of the Sprayed Panicles"; pp. 567–75 in *Thermal Spray: A United Forum for Scientific and Technological Advances*. Edited by C. C. Berndt. ASM International, Materials Park, OH, 1997.

<sup>20</sup>C. Meterns-Lecomte, D. Muck, and J. Garcia, "Characterization of a New Aerospace Thermal Barrier Coating"; pp. 61–65 in *Thermal Spray Industrial Applications*. Edited by C. C. B. A. S. Sampath. ASM International, Materials Park, OH, 1994.

<sup>21</sup>D. Sacriste, N. Goubot, J. Dhers, and A. Vardelle, "Optimization of Thermal Barrier Coatings Sprayed by the Plazjet Plasma Gun"; pp. 550–55 in *United Thermal Spray Conference—1999*. Edited by E. Lugscheider and P. A. Kammer. German Welding Society, Dusseldorf, Germany, 1999.

<sup>22</sup>N. Goubot, J. Dhers, and M. Ducos, "Comparison of TBC Coatings Obtained by Conventional and High Velocity Plasma Spraying"; pp. 556–60 in *United Thermal Spray Conference—1999*, Edited by E. Lugscheider and P. A. Kammer. German Welding Society, Dusseldorf, Germany, 1999.

<sup>23</sup>A. Haddadi, F. Nardou, A. Grimaud, and P. Fauchais, "Generation of the First Layers of a Zirconia Plasma Sprayed Coating: Correlation Between Splat Layering and Spraying Parameters"; pp. 249–54 in *Thermal Spray Science and Technology*. Edited by C. C. Berndt and S. Sampath. ASM International, Materials Park, OH, 1995.

<sup>24</sup>S. Sampath, X. Y. Jiang, J. Matejcek, A. C. Leger, and A. Vardelle, "Substrate Temperature Effects on Splat Formation. Microstructure Development and Properties of Plasma Sprayed Coatings: Part I: Case Study for Partially Stabilized Zirconia," *Mater. Sci. Eng. A*, in press. □